



New empirical relationship between resonance frequency and thickness of sediment using ambient noise measurements and joint-fit-inversion of the Rayleigh wave dispersion curve for Kangra Valley (NW Himalaya), India

Praveen Kumar¹ · Ambrish Kumar Mahajan¹

Received: 26 January 2019 / Accepted: 14 May 2020 / Published online: 25 May 2020
© Springer-Verlag GmbH Germany, part of Springer Nature 2020

Abstract

Northwest Himalaya is one of the seismically active regions that had experienced a number of major and moderate earthquakes in the past. The 4th April 1905 Kangra earthquake (M_s 7.8) is one amongst those which had caused a devastating effect to the built environment, as a consequence of amplification factor due to varied impedance contrast between the overlying alluvial soil and underlying bedrock. Preventive actions aimed at minimizing the economic losses caused by such events require estimation of dynamic characteristics of the surface soil and its behaviour under strong motion excitation. Under this initiative, the Kangra Valley, which falls in seismic zone IV and V, was extensively studied to elucidate the effects of earthquake excitation on the built environment due to the soil amplification. The Kangra Valley is characterized by the presence of hills and valleys, thus has a very high variation in the sediment thickness above bedrock which is an important parameter for seismic hazard assessment. This study aims to establish a new empirical relationship from the experimental data for estimating sediment thicknesses of the Kangra Valley. Under this initiative the resonance frequency has been calculated from ambient noise measurement from 200 sites of the Kangra Valley. This extensive survey allowed the estimation of resonance frequencies (4–20 Hz) in the region and identified the areas prone to site amplification. Furthermore, joint-fit-inversion modelling of horizontal to vertical spectral ratio (HVSr) and dispersion curves obtained from ambient noise measurement and multichannel simulation with one receiver (MSOR) data acquisition, respectively, led to 1-D shear wave velocity (V_s) profile. New empirical relationships were established for Kangra Valley to estimate the thickness of overburden using non-linear regression analysis between resonance frequency (f_0) obtained by HVSr technique and pseudo-depth (H) from the study area. The equation provides an effective tool to detect sediment thicknesses in the area with similar geological setup. The methods described in the study apply a new approach to derive new empirical relationship in hilly terrain and the area with sparse borehole record.

Keywords Ambient noise measurement · Resonance frequency · Multichannel simulation with one receiver (MSOR) · Sediment thickness estimation

Introduction

Site characterization is one of the main requirements to understand the behaviour of seismic waves during strong motion excitation. It provides a major input to ascertain

basin characteristics for hazard zonation and risk assessment studies. Over the years, the damage distribution during an earthquake reveals the significance of local geology and thickness of soft sediments. The extent of damage in the frontal part of the Himalaya, during the 2005 Kashmir earthquake (M_w 7.6) and 2015 Nepal earthquake (M_w 7.8) also demonstrated the deleterious effects of loose alluvial soil (Mahajan et al. 2006; Chan et al. 2017; Gautam 2017). Thus, estimating the thickness of soft sediments above bedrock and its impedance contrasts are of major concern in the frontal part of the Himalaya. The Kangra Valley is one such region

✉ Praveen Kumar
pk.hpkv@gmail.com

¹ Department of Environmental Science, Central University of Himachal Pradesh, Dharamshala, Himachal Pradesh 176215, India

in the Northwest Himalaya that had suffered major effects from the 4th April 1905 (Ms 7.8) Kangra earthquake, and according to the Middlemiss (1910) report, a varied degree of damage within the same intensity zone (intensity X on Rossi–Forel scale) was reported from different parts of the valley, which indicates the influence of the varied thickness of the sediment. The seismic zonation map of India reveal the region falls in seismic zone IV and V with very high seismic hazard potential (BIS 2002). According to the seismic hazard analysis, the Kangra region can have a peak ground acceleration (PGA) of 0.50 g with 10% probability of exceedance in 50 years (Mahajan et al. 2010). Thus, to understand the effects of near surface material on strong ground motions in such a seismically active region with varied lithology, complex geology and varied thickness of sediments, a detailed mapping of bedrock depth and thickness of soft soil is required. The aim of this study is to estimate the thickness of soft sediments using horizontal to vertical spectral ratio (HVSr or H/V) analysis and multichannel simulation with one receiver (MSOR) data modelling and thereafter to establish new empirical relationship to derive thickness of sediment above bedrock. Since the thickness of sediment is linked with the frequency and stiffness of the soil column, efforts were made to measure the fundamental/resonance frequency (f_0) and shear wave velocity (V_s) of each soil column.

The resonance frequency of the soil column was derived using ambient noise measurements. The concept of recording ambient noise measurements was first proposed by Kanai (1961), Kanai and Tanaka (1961) and Nogoshi and Igarashi (1971) for spectral analysis, and later improved by Nakamura (1989, 2000) by normalizing the source effect through horizontal to vertical spectral ratio (HVSr). Presently, the technique is being used worldwide as a low-cost and effective tool for estimation of resonance frequency (f_0) and amplification (A) characteristics, although the theoretical background of HVSr technique is debatable, while some studies have even demonstrated the good consistency between the estimates derived from ambient noise and earthquake records (Bindi et al. 2000; Fah et al. 2001; Chan et al. 2017). Many researchers have provided critical reviews on the application of HVSr technique (Al Yuncha and Luzon 2000; Bindi et al. 2000; Mucciarelli and Gallipoli 2001; Bonnefoy-Claudet et al. 2006; Lunedei and Malischewsky 2014). Parolai et al. (2002) and Tun et al. (2016) confirmed that the HVSr technique provides a good estimate of the fundamental frequency if there is clear impedance contrast between soft soil and bedrock.

The shear wave velocity (V_s) is another input required for subsurface characterization that can be calculated using different geotechnical and geophysical methods. Traditionally, geotechnical investigations are generally carried out using standard penetration test (SPT) and borehole investigations,

to provide information on the subsurface material properties. However, for the present study area, these techniques seem to provide erroneous results, because the valley is underlain by fan sediments, mainly consisting of gravels, pebbles and boulders, which are unsuitable for performing standard penetration test. Therefore, detailed site characterization was planned using seismic data collection in active and passive mode. The passive mode of data acquisition records ground vibrations which are present in the environment (e.g. microseisms and microtremors), whereas the active mode acquires the seismic data using multichannel simulation with one receiver (MSOR) mode. The MSOR is a modified version of the multichannel analysis of surface waves (MASW). It uses an active excitation source and requires a single sensor and trigger for data collection rather than a set of geophones like that of MASW data acquisition (Harutoonian et al. 2013). Thus, during seismic data acquisition, a velocimeter fixed at a location of interest allows us to estimate resonance frequency using HVSr technique and the same instrument can be used to gather Rayleigh wave dispersion characteristics through the MSOR technique at the same observation point. Since the Kangra Valley has rugged topography, finding flat open ground at every location was difficult, which limits the possibility of conducting shear wave velocity investigation using MASW. So, simultaneously, MSOR was used on small ground surfaces for deriving one-dimensional (1-D) shear wave velocity profile using joint-fit-inversion modelling of HVSr and dispersion curve. Moreover, at sites where even minimal linear profiles of MSOR survey could not be performed, only resonance frequencies were measured using ambient noise measurements (Fig. 1).

To obtain a one-dimensional (1-D) shear wave velocity (V_s) profile, base information on the thickness of near surface top soil layer is required, which can be achieved by different techniques like seismic reflection, multichannel simulation with one receiver (MSOR) and multichannel analysis of surface waves (MASW). The MSOR as well MASW techniques are not capable of providing information down to depths greater than 40 m; however, passive mode of data acquisition using HVSr can provide deeper information about the subsurface material from the joint-fit-inversion modelling of the HVSr curve. Finally, new empirical relationships have been established for the Kangra Valley between resonance frequency and thickness of sediment. This newly established relationship will also be helpful in estimating the thickness of those areas which have only information about resonance frequency due to the presence of forest cover or high hill slopes.

Geology and tectonics

The Kangra Valley is a piggyback intermontane basin, which is approximately 75 km long and 10–25 km wide (Ori and Friend 1984; Thakur et al. 2014) formed in the

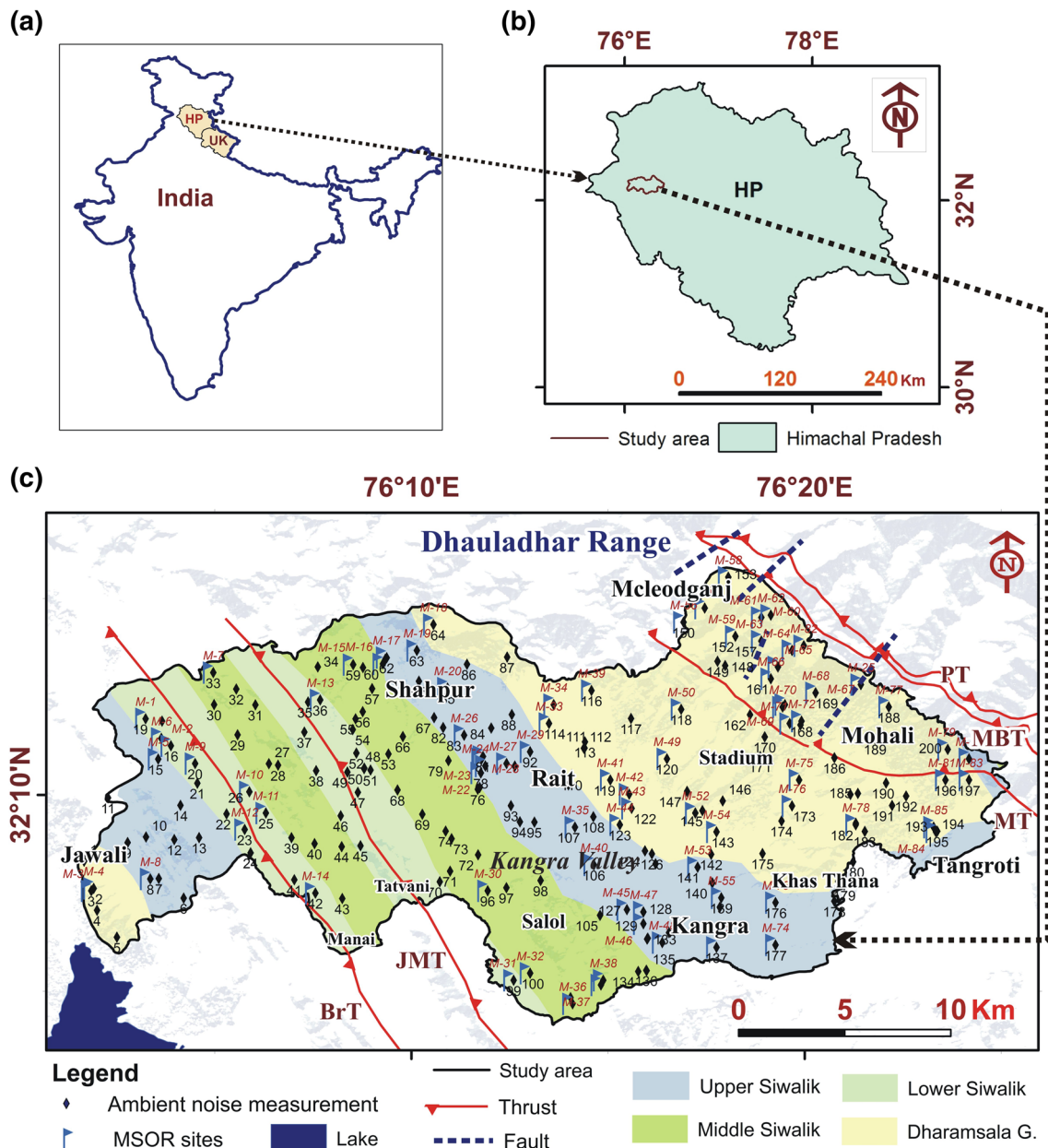


Fig. 1 Location map of the study area with respect to **a** India and **b** Himachal Pradesh, showing, **c** the sites of ambient noise measurements (200) and MSOR (85) data collection on the geo-tectonic map

of Kangra Valley. *BrT* Barser back thrust, *JMT* Jawalamukhi thrust, *MBT* main boundary thrust, *MT* Murree thrust, *PT* Panjal thrust

Outer Himalayan region of Northwest Himalaya (Fig. 1c). The valley to the north is bounded by the steep range of Dhauladhar Mountain and Lesser Himalayan rocks, whereas the southern part is characterized by geomorphic features like ridges, valleys and small mountain peaks of the Outer Himalayan range. The ridges are underlain by tertiary rocks (Sandstone and Upper Siwalik Boulder Conglomerates) or glaciated moraine deposits and overlain by alluvial sediments, whereas valleys are underlain by fan sediments of varied thickness. Tectonically, the valley is marked by the

presence of major thrust systems due to the continuous northward movement of the Indian landmass. The valley is sandwiched between two major tectonic features, i.e. the Jawalamukhi thrust (*JMT*) to the south and the main boundary thrust (*MBT*) to the north (Thakur et al. 2014; Jayangondaperumal et al. 2017; Fig. 1). Steeply dipping faults also traverse the area, which extend from the Outer Himalayan to Lesser Himalayan zone. Many of these faults are conjugate wrench faults striking approximately NNE–SSW (Mahajan and Kumar 1994). The valley also represents a

unique example of evolutionary history of Quaternary Fan deposits that pass through an interval of several climatic oscillations (glacial and interglacial; Sah and Srivastava 1992). The presence of active tectonic features provides an indication of major contributions from tectonically driven erosional processes (Dey et al. 2016). The continued erosion and deposition of sediments in the frontal part of Himalaya lead to the formation of fan deposit in the lowland area. The vertical lithological profile of the Kangra Fan area shows the dominance of gravels in litho-facies, which is further characterized by the presence of glacial moraines and clay-rich debris-flow deposits in the upper fan area, sandy fill deposits in the middle fan and sand, silt and mud deposits in the lower fan areas (Sah and Srivastava 1992). The Quaternary sediments (clay, gravel and boulder) present in the area can play a crucial role in strong motion excitation.

Methodology

The ambient noise measurements were recorded from 200 sites in the Kangra Valley to derive the resonance frequency (f_0) (Fig. 1). Among these, 85 sites were covered using both the multichannel simulation with one receiver (MSOR) technique and ambient noise measurements and the HVSR curves derived from these sites can be modelled using joint-fit-inversion of HVSR and dispersion curve. Finally, the HVSR data and the thickness derived using inversion analysis were used to obtain a new empirical relationship between resonance frequency and thickness of the soil column.

Data acquisition and processing of ambient noise

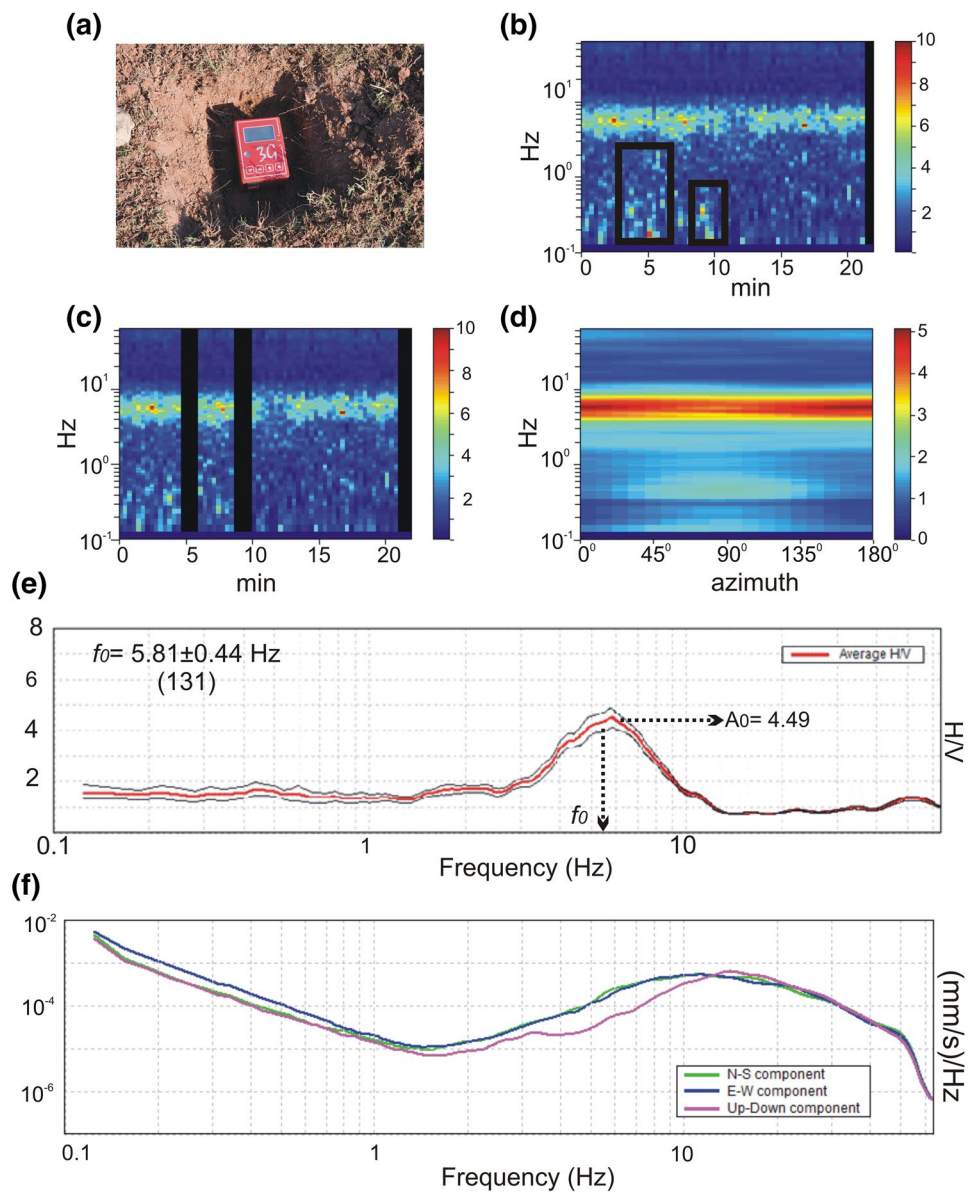
Extensive ambient noise measurement survey was carried out covering the entire Kangra Valley within and along the fringes of the Kangra basin. The instrument used is a tromograph named “Tromino” (model ENGY), consisting of a three component electro-dynamic sensors having an operating frequency range of 0.1–1024 Hz. Better coupling of the instrument with ground was ensured by fixing the instrument using three long spikes. The instrument was set up inside a pit to avoid any interference from direct wind noise or footsteps, etc. (Fig. 2a). The data were acquired for 20 min with a sampling frequency of 128 Hz, considering the SESAME (Site EffectS assessment using AMBient Excitations) criteria (SESAME 2004). The acquired data was imported and analysed using ‘Grilla’ software (Fig. 2b–f). The ambient noise measurement records were analysed in 60 non-overlapping time windows of 20 s with different smoothing techniques, i.e. triangular window (TW), cosine window (CW), rectangular window (RW) and Konno and Omachi window (KO) with b value = 40 (Konno and Omachi 1998). The data processing was performed in the frequency

range of 0.2–60 Hz, but only the peaks within or close to the 0.2–30 Hz were considered for the study purpose. Different smoothing techniques were attempted and finally the triangular window (TW) filtering was applied to all the data set, thus reducing the standard deviation (SD) of H/V spectral ratio for better discrimination of stratigraphic peaks. The HVSR analysis led to single or multiple frequency peaks and the frequency with maximum amplitude was marked as ' f_0 ' and the corresponding amplitude as ' A_0 '. The sites with secondary and tertiary peak also had distinctive frequencies which were denoted as ' f_1 ' and ' f_2 ' with amplitude ' A_1 ' and ' A_2 ', respectively (Fig. 3a). The peak with maximum amplitude (A_0) was used to select the main resonance frequency (f_0) of the site. The resonance frequency was selected in the frequency band of engineering interest (0.5–20 Hz), which, in Fig. 3a, falls within the dotted green rectangle, while the higher frequency range (> 20 Hz) in the red dotted rectangle represents a very shallow contrast and so generally excluded from the final analysis. The noisy transients were removed during final processing to get clear spectrum peaks that further helped to distinguish anthropic peaks (dirac like) from stratigraphic one ('eye' shaped structure in spectral amplitude curves; Fig. 3b).

The removal of noisy transient from the time window (Fig. 2b, c) provides a clearer HVSR curve. After identifying the stratigraphic peaks, the corresponding H/V curves were checked using SESAME criteria that define conditions for clear and reliable identification of H/V peaks (SESAME 2004; Rezaei et al. 2013; Gabas et al. 2014; Rezaei and Choobbasti 2017; Mahajan and Kumar 2018). The H/V curves were also used to identify different layers with significant impedance contrast, in case of curves having more than one peak. From this check, the identification of peaks found at some of the sites showed less reliability, as per SESAME criteria, so such sites were excluded from the final analysis.

The HVSR technique has a lot of applications including identification of the resonance contrast between sediments and the bedrock comprising variable stratigraphic succession (Ansal 2004; Tarabusi and Caputo 2016; Gosar 2017; Mi et al. 2019). The HVSR peaks were used to select dominant velocity contrast between the overlying soft sediments and underlying stiff strata/bedrock. The analysis further reveals that the Kangra Valley is marked by different typologies of HVSR curves (i.e. broad, clear and flat peak). Clear HVSR peaks were identified in the central part of the study area, where sharp contrast is observed between the overlying soft sediment and the underlying stiff sediment (Fig. 4a). Broader HVSR peaks are observed in the regions that are characterized by sloping interface or shallow structures (i.e. the JMT) between softer and very stiff material (i.e. site no. 49; Fig. 4b). Multiple HVSR peaks were observed in the areas having moderate topographic relief that are characterized by multiple contrast. These multiple contrasts may be due to the material

Fig. 2 Example of ambient noise measurement in passive mode; **a** field setup showing Tromino in a ~0.07 m deep pit; **b** time variation of the frequency component with rectangular frames marking the disturbance related with transient noise, **c** which was further removed from the HVSR analysis; **d** directional HVSR with colour showing the amplitude of HVSR spectra; **e** HVSR curve and **f** amplitude spectra of the three components



composition of the Dharamsala Group of rocks, which consists of claystone, mudstone and sandstone (Fig. 4c). Flat HVSR curves were observed from some of the isolated locations that are characterized by hard bedrock lithology, mainly Middle Siwalik Sandstone and Upper Siwalik Boulder Conglomerates (Fig. 4d; site no. 183).

The presence of fan sediment subsurface lithology made it difficult to get a clear peak at low frequency, because of very low impedance contrast between the underlying bedrock and overlying fan sediments.

Multichannel simulation with one receiver (MSOR) data acquisition

The MASW technique deploys multiple receivers laid down along a linear array connected to a common recorder [analog-to-digital (A/D) convertor] named as engineering seismograph. The multichannel data acquisition requires a relatively long spread (100–150 m) on ground to penetrate deeper, as in general, the penetration depth is equal to half of the spread length, although it also depends on three factors,

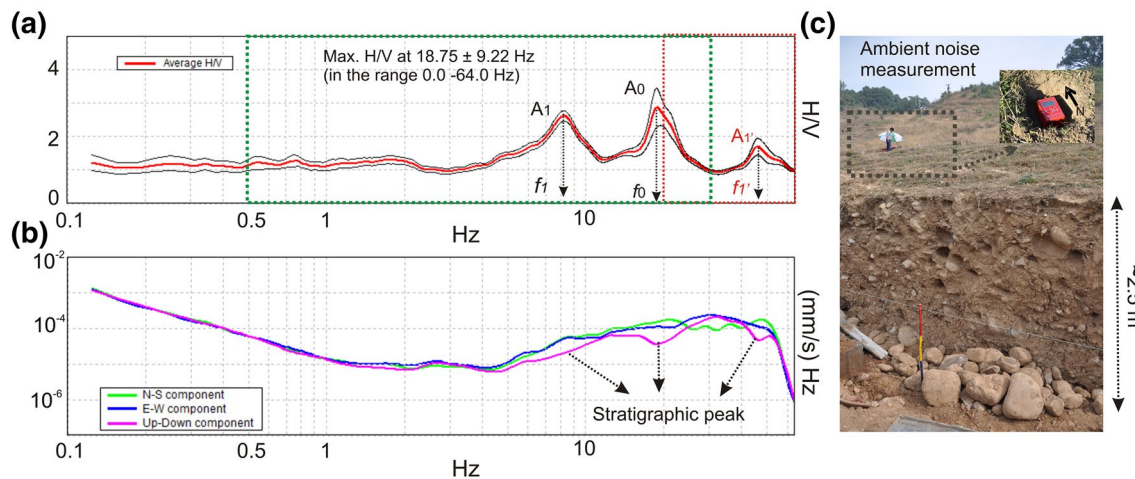


Fig. 3 Multiplicity of HVSR peak (site no. 139-II) with subsurface heterogeneities; **a** HVSR peak with distinctive frequency (f_0 , f_1) and amplitude (A_0 , A_1); **b** corresponding stratigraphic peaks with ‘eye’

shaped structure in up-down component; **c** site condition showing subsurface heterogeneities (boulders) excavated from the area

i.e. impact source energy, frequency of geophone and the stiffness of the material underneath (Mahajan 2009). In the frontal part of Himalaya, where large open grounds are not easily available, instead of using MASW, the MSOR mode of data acquisition was used to obtain information on shear wave velocity from the Rayleigh wave dispersion curve. Due to irregular topographic conditions, depth of bedrock varies from a few meters to tens of meters. The MSOR technique can be used on smaller area as shown by various authors (Ryden et al. 2004; Tokshi et al. 2013; Lin and Ashlock 2016). The technique relies on active excitation of seismic waves recorded by a single receiver and a trigger geophone, instead of relying on a set of geophones as per the MASW technique. In hilly terrains, the use of MSOR was found much more advantageous than MASW in term of speed, portability and space. The same tomograph has been used in active and passive mode for recording seismic waves using a combination of analysis methods for subsoil velocity modelling (Harutoonian et al. 2013). The impact source and trigger were moved with respect to the sensor in an incremental manner to cover a 1-D array of ~20–25 m on ground (Fig. 5). From each excitation, seismic traces were acquired and finally, combining all individual seismic traces, a simulated multichannel record was compiled for further processing (Fig. 6). The seismic traces were processed using ‘Grilla’ software to generate a dispersion image in the form of an overtone image (Fig. 6f).

The dispersion curves obtained using MSOR can have fundamental and higher modes, whereas in MASW technique, mostly the fundamental mode is obtained and used for dispersion analysis. The overtone image of the dispersion curve represents three variables, i.e. phase velocity versus frequency, while colour represents the amplitude of the

signal, which is a function of wavelength (λ), as the maximum depth (Z_{\max}) for which shear wave velocity (V_s) can be reasonably calculated (Rix and Leipski 1991).

Combining the dispersion curves derived from MSOR and the H/V curves from ambient noise analysis, a joint-fit-inversion modelling was performed using the Occam’s razor principle that suggests to select the minimum number of model parameters, with a number of peaks (n) and layers ($n + 1$) to be used for a reliable result. The dispersion curve obtained from the MSOR technique provided the initial information on phase velocity and phase frequency. According to Kramer (1996), the fundamental frequency (f_0) is a function of shear wave velocity (V_s) and thickness (H) of the soil column according to the relation:

$$f_0 = V_s/4H. \quad (1)$$

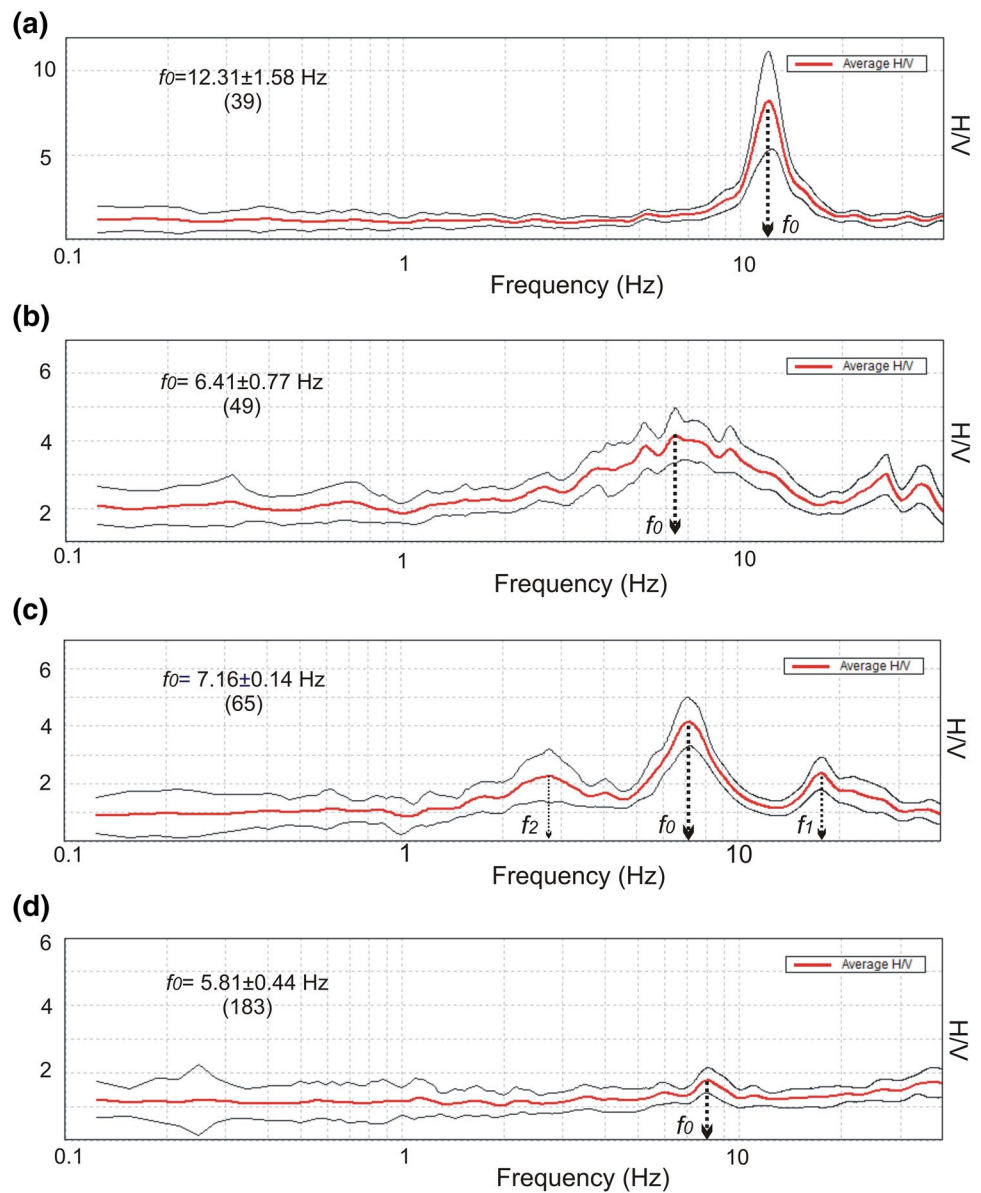
So using this equation, one can derive the thickness of the soil column if the shear wave velocity of that soil column is known, which could be derived by collecting the seismic data using either the MASW or the MSOR technique.

Results

Joint-fit-inversion modelling

To estimate the approximate depth of the first impedance contrast responsible for resonance in the frequency range of engineering interest (<20 Hz), the phase velocity spectra derived using MSOR technique were used to provide constraints to the inverse modelling procedure of the HVSR curve. This modelling was based upon the assumption of

Fig. 4 Different typologies of HVSR curve; **a** clear, **b** broad, **c** multiple and **d** flat HVSR peaks in Kangra Valley



plane parallel stratigraphy, so the presence of lateral heterogeneities can lead to incorrect interpretations of phase velocity spectra. The first HVSR peak below 20 Hz was modelled using the information of thickness and shear wave velocity from the dispersion curve. The second HVSR peak was modelled with the support of the same phase velocity spectra. Further, low frequency HVSR peaks of the same curve were further modelled using trial and error method. During the inversion procedure, the synthetic HVSR curve obtained from initial modelling was matched with the experimental average HVSR curve (e.g. Castellaro and Mulargia 2009; Roser and Gosar 2010). The modelling of the higher mode were taken into consideration in estimating the thickness of shallow layer. The best fitting criterion between experimental and synthetic HVSR curves was used in inversion

analysis after taking base information of shear wave velocity of the soil type from the dispersion curve (Fig. 7a, b).

In the present study, the medium frequency HVSR peaks (3–10 Hz) are dominant, while the HVSR curves sometime become more chaotic and irregular towards the ends. At few locations, the HVSR peaks were almost flat maybe because of the presence of material properties and near surface bedrock which bring impedance contrast very low.

Figure 7a shows the H/V curve of the site located in the extreme southern part of the valley with HVSR peak at 6.81 Hz (site no. 36). The dispersion curve obtained from the same site using MSOR survey shows a phase velocity (c) of 430 m/s corresponding to phase frequency (f) of 8.0 Hz. Since, the penetration depth (Z_{max}) is half of the wavelength (λ), where $\lambda = c/f$, i.e. $430 \text{ m/s}/8.0 \text{ Hz} = 53.75 \text{ m}$, thus the

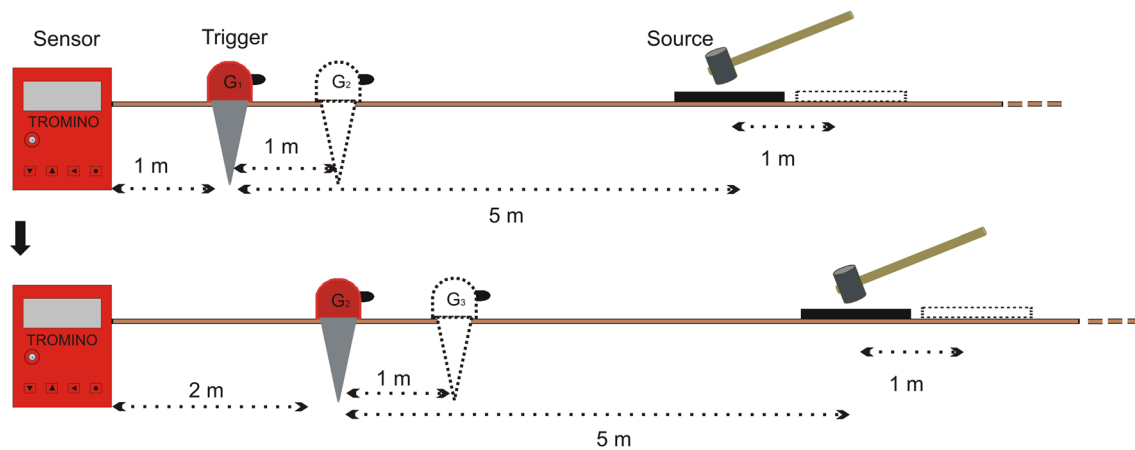
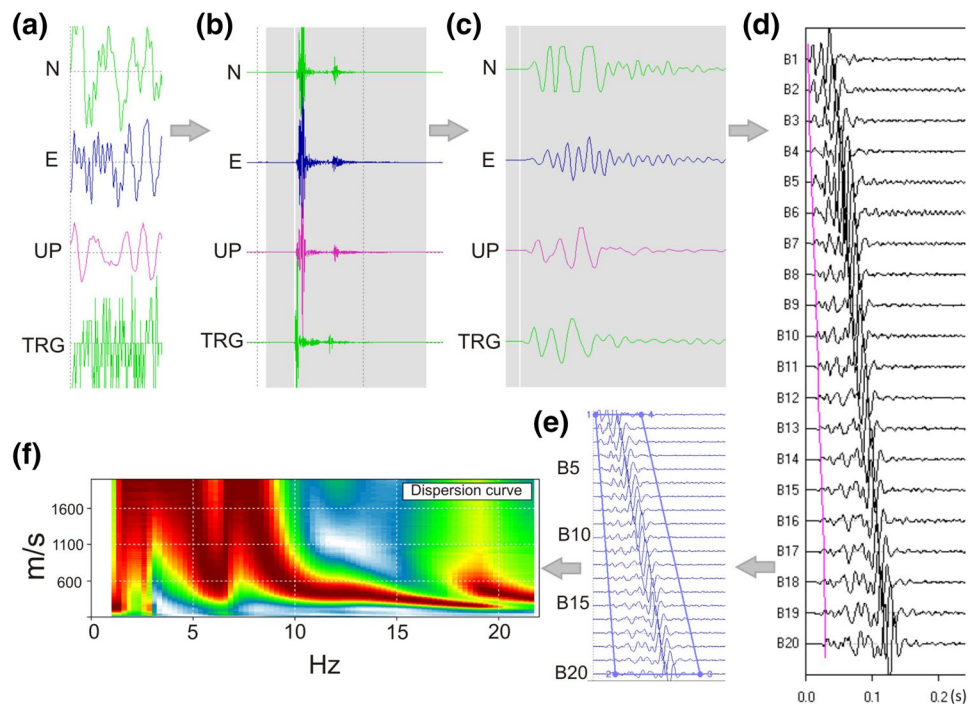


Fig. 5 Schematic diagram of field configuration for data acquisition using multichannel simulation with one receiver (MSOR) mode, showing location of sensor, trigger and source with respect to each

other. The dotted geophone and plate show their next location while acquiring data in an incremental manner

Fig. 6 Processing steps of multichannel simulation with one receiver (MSOR) data using ‘Grilla’ software: **a** acquired raw data along different channels, **b** picking of first arrival, **c** picking of shot times with respect to trigger channel, **d** combining different multiple records in a single seismic record, **e** selecting an appropriate portion of signal and **f** generation of dispersion curve



penetration depth achieved is ~ 27 m (Fig. 7b). In Fig. 7, the frequency band 8–14 Hz corresponds to the higher mode and the input from array and HVSR were used in the joint-fit-inversion modelling. The first predominant HVSR peak provides the shallower contrast at a depth of 6 m, which is in good agreement with the shear wave velocity (V_s) profile obtained from MSOR data. The maximum penetration depth deduced by the MSOR survey is marked by red dotted line (Fig. 7c), whereas the velocity model was extended by inverting the low frequency peaks of the HVSR curve (Castellaro and Mulargia 2009; Castellaro 2016; Gupta et al.

2019). Another site located in the central part of the valley shows the HVSR peak at 4.97 Hz (site no. 103; Fig. 7d), and the maximum depth of penetration achieved using MSOR survey is estimated to be ~ 28 m, i.e. resulting from $c = 386$ m/s and $f = 7.0$ Hz (Fig. 7e, f). The joint-fit-inversion modelling of HVSR and dispersion curves provide shallow depth information (Fig. 7f). The third site (site no. 144), from the northern part of Kangra Valley, shows the main peak was at 11.88 Hz (Fig. 7g). The analysis of dispersion curve allowed to achieve a maximum depth penetration of 30 m (Fig. 7h), whereas the inversion of HVSR low

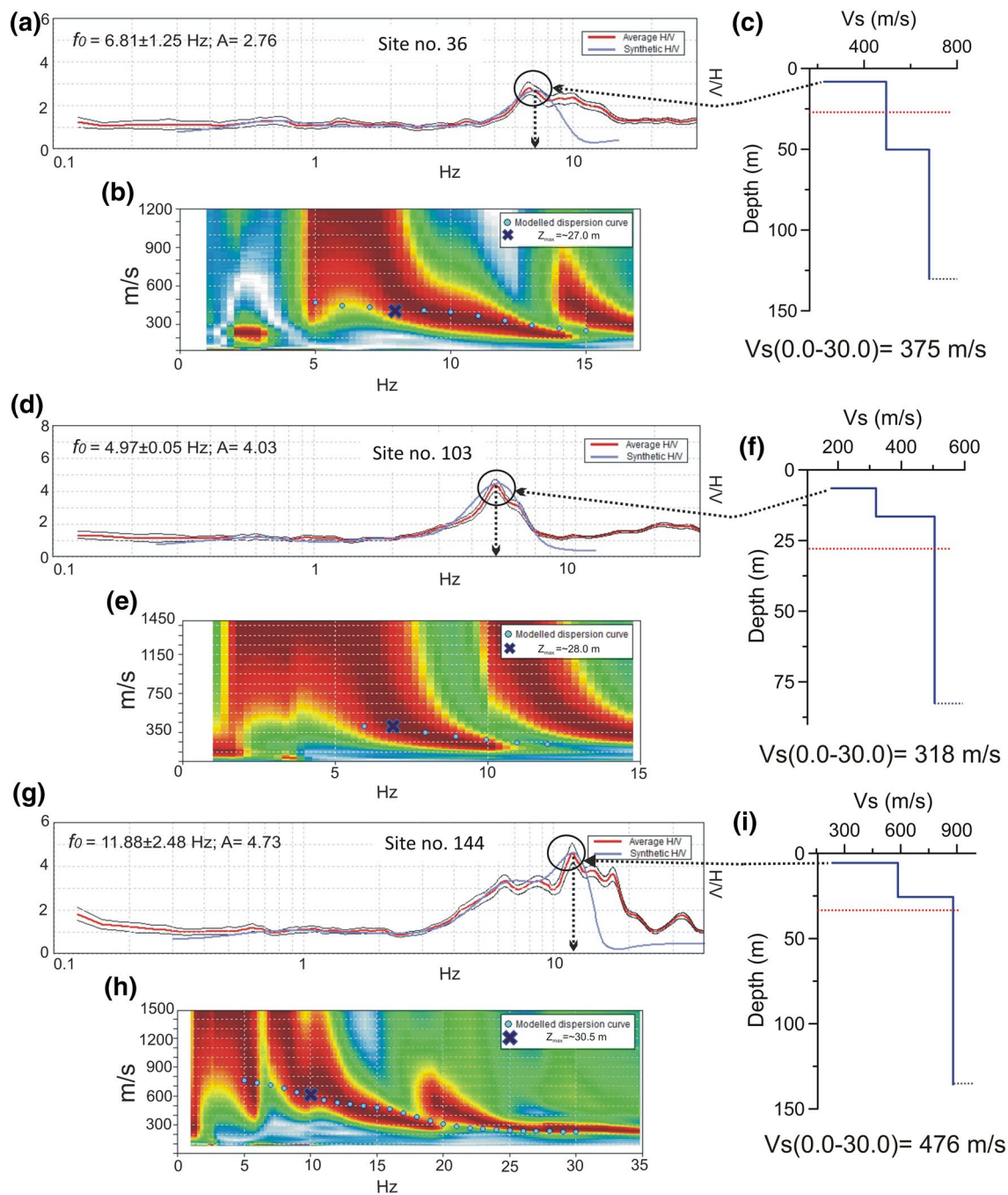


Fig. 7 Diagrams showing the outcome of the joint-fit-inversion modelling for three different sites, with modelled HVSR curves (a, d, g), MSOR driven dispersion curves (b, e, h) and correspondingly derived

1-D shear wave velocity profiles (c, f, i). Red dotted lines mark maximum penetration depths deduced by the MSOR survey

frequency peaks allowed to investigate up to 75 m depth (Fig. 7i).

New empirical relationships between f_0 and H

The Kangra Valley is highly rugged and criss-crossed by southern flowing drainages due to the presence of ridges and

valleys. The valley is underlain by fan sediments, whereas the ridges are underlain by either tertiary sedimentary rocks or moraine (glacial) deposits. Under such conditions covering all sites using MASW or MSOR was not feasible due to non-availability of space for longer linear profile. However, conducting ambient noise measurement was possible even in such locations. In such area, site characterization has been

achieved by establishing an empirical relationship between fundamental frequency and pseudo-depth (H), defined as the empirically estimated depth of the main impedance contrast. A number of empirical relationships between fundamental frequency and pseudo-depth were previously established for different regions of the world by various authors, i.e.:

$$H = 96f_0^{-1.388}, \tag{2}$$

for the Lower Rhine Embayment in Germany (Ibs-von Seht and Wohlenberg 1999)

$$H = 108f_0^{-1.551}, \tag{3}$$

for the Cologne area—Germany (Parolai et al. 2002)

$$H = 105.99f_0^{-1.1531}, \tag{4}$$

for the coast South of Istanbul (Birgoren et al. 2009)

$$H = 141f_0^{-1.27}, \tag{5}$$

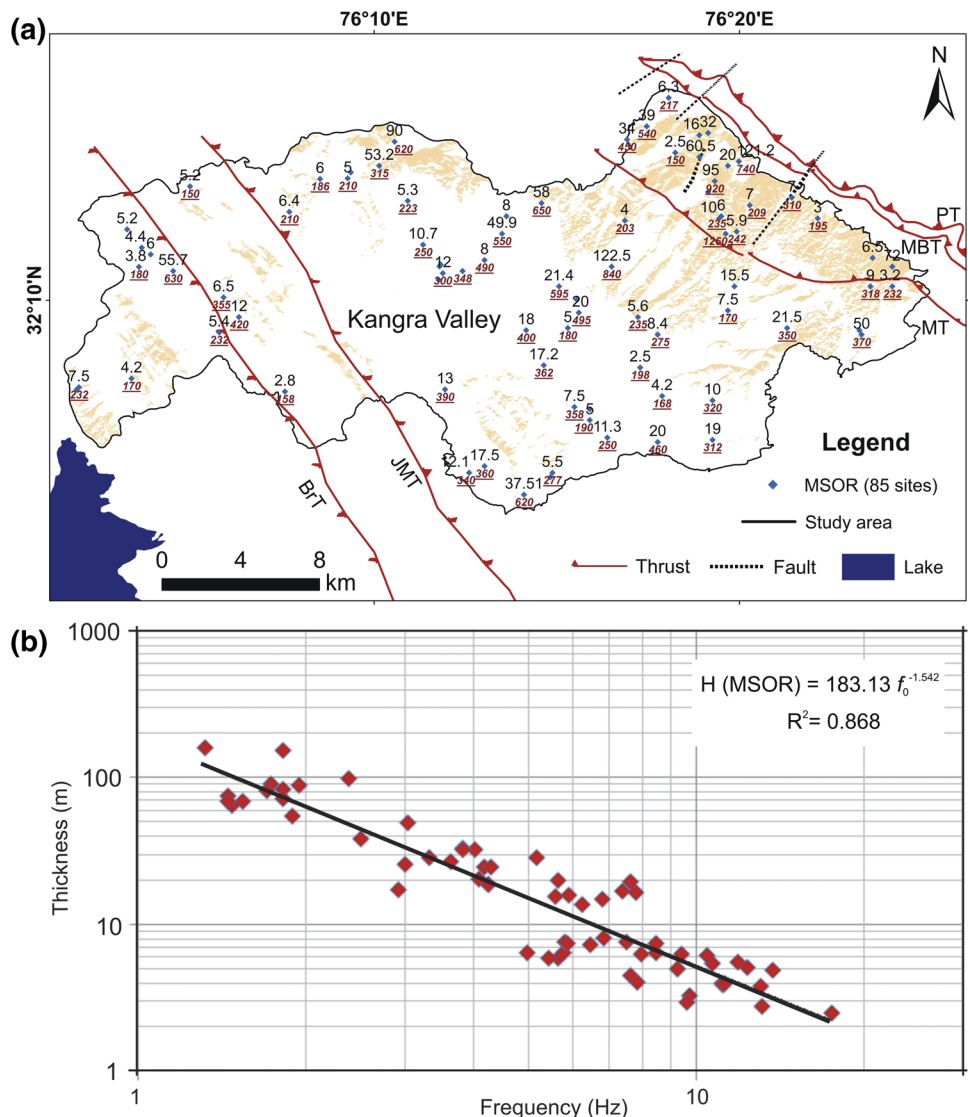
for the Izmit Bay area—Turkey (Ozalaybey et al. 2011)

$$H = 146.01f_0^{-1.2079}, \tag{6}$$

for the Kathmandu Valley—Nepal (Paudyal et al. 2013).

Most of these equations were obtained using rigorous geophysical investigations and their comparison with borehole record, whereas for the present study area, limited information was available from sparse borehole records, so the thickness of each layer and its shear wave velocity was derived using surface wave analysis and joint-fit-inversion modelling. Thus, to calculate the sediment thicknesses, the use of area specific shear wave velocity and thickness have been used for reliable results. In the present study, the thickness of sediments derived using joint-fit-inversion modelling of HVSR and dispersion curve was plotted against the

Fig. 8 **a** First order pseudo-depth with respect to the main contrast (black numbers) and the respective shear wave velocity (red numbers) from the modelled HVSR peak. **b** Plot of thickness versus resonance frequency derived from joint-fit-inversion and ambient noise measurements, respectively; solid line shows the non-linear fit to derive an empirical relationship between fundamental frequency and experimental pseudo-depth (H) as Eq. 7



fundamental frequency (f_0) of 85 sites for which HVSR and MSOR data were available (Fig. 8).

Although due to physiographic constraints, the MSOR data points are not homogeneously distributed, however the HVSR and MSOR measurements from 85 sites gave enough data to derive a new empirical relationship for the study area through a non-linear regression analysis between thickness and resonance frequency. The fundamental frequency derived for 85 sites was plotted against thickness of sediment and the resulting equation is

$$H(\text{MSOR}) = 183.13f_0^{-1.542}. \tag{7}$$

The thickness of sediment at a particular site along with their shear wave velocity with respect to the main contrast is shown in Fig. 8a, whereas the Fig. 8b shows the non-linear regression fit between fundamental frequency and sediment thicknesses. The final equation derived from experimental data was used for calculating the thickness of sediment of other sites, where it was not possible to acquire data with MSOR as well MASW. Thus, it has been concluded that in the absence of any shear wave velocity data, thickness of sediment can be derived using fundamental frequency of that site and applying the same in Eq. 7. Further to compare our results the present study data has been plotted in double logarithmic coordinates as shown in Fig. 9 using different empirical relationship of the world. The empirical relationship for this study between fundamental frequency and depth shows good fitting with the derived regression curve ($R^2 = 0.868$). In a double logarithmic plot, the slope is represented by 'b' value, whereas 'a' value represents the y intercept. The 'b' value of Kangra Valley is found to be significantly higher than in other regions of the world except Germany (Ibs-von Seht and Wohlenberg 1999; Parolai et al. 2002). The higher 'b' value of the study region could be due to variability in the thickness of sediment and the shear wave velocity parameters. Actually, in several studies the resulting b values were found close to -1, but for the Kangra Valley (and the Cologne zone in Germany) 'b' is around -1.5,

which implies that thickness decreases with the increase of the resonance frequency more rapidly than what expected for horizontal homogeneous layers. This can be due to the fact that local conditions can differ from those of a soft horizontal homogeneous layer overlying a stiff bedrock, thus causing resonance frequencies modified by 2D/3D effects and/or lateral variations of Vs. On the basis of shear wave velocity, in Kangra Valley three types of lithology can be distinguished, namely, the bedrock having shear wave velocity of the order of > 760 m/s, moraine sediments having an average shear wave velocity of the order of 450–500 m/s, fan sediments and alluvial soil having an average shear wave velocity of the order of 200–300 m/s (Mahajan and Kumar 2018).

Based on Eq. 7, the spatial distribution of thickness value in the study area is shown in Fig. 10. According to this map the thickness of the alluvial sediments is very thin the northern part of the basin and are underlain by hard rock (sandstone or Upper Siwalik Boulder Conglomerate), thus the impedance contrast is very high in such area especially in the northern part of the valley. The north-central and central part of the basin have thick sedimentary fans but the constituents of these sediments are as that of Upper Siwalik Boulder Conglomerate, thus having a low velocity contrast between the overlying layer and underlying hard rock. Therefore, HVSR peak frequency (f_0) of these sites have almost flat HVSR curve in contrast to the northern and south-western area which is characterized by hard rock underlying alluvial sediments. Some of the sites are directly exposed on the surface or have very-very thin alluvial cover, thus it has found that the sediment thickness estimated using Eq. 7 of such sites is found to be overestimated (encircled in Fig. 10) as compared to other sites of the basin.

Discussion and conclusion

Although, Kangra Valley had experienced a devastated effect during 1905 Kangra earthquake (Ms 7.8; Ambraseys and Douglas 2004), since then most of the frontal part of

Fig. 9 Different fitting curves and the obtained empirical equation for the Kangra Valley

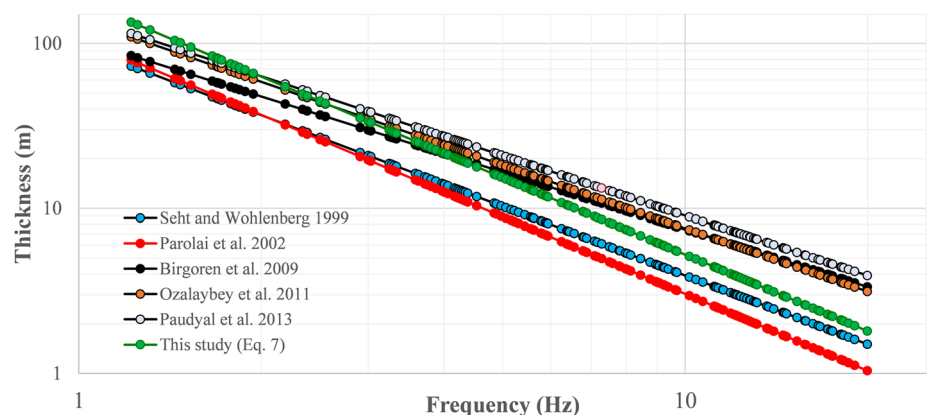
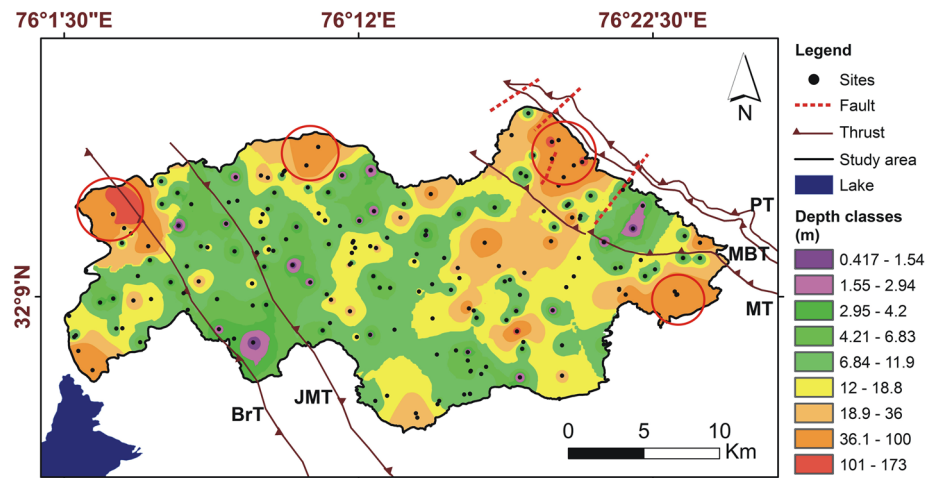


Fig. 10 First order pseudo-depth derived using new empirical relationship for the Kangra Valley



Himalayan region has witnessed unplanned urbanization which is prone to site amplification. The reported variation in the damage within the valley and on the fringes of the basin and upcoming non-resistant construction activity in the region prompted us to carry out site characterization studies. Since the properties of the near surface material are required for estimating site amplification parameters of the Kangra Valley, the present study was planned to give insight into the needs of seismic resistant structures to reduce the impact of future earthquakes. Until today, most of the Himalayan frontal belt is marked under seismic zone IV and V, based on the damage distribution of previous earthquakes. There are no data on the thickness of the soil column and its shear wave velocity by virtue of which one can calculate the seismic parameters for the site response analysis. Thus, efforts were made to estimate the shear wave velocity and thickness of each site using seismic method. A new empirical relationship has also been established for the Kangra region to cover those sites where topographic and physiographic hurdles prevent long seismic profiling. The study revealed that the applications of joint-fit-inversion modelling can be very useful in estimating the shear wave velocity parameters of different sites in the frontal part of the Himalayan region, because it needs much less space and is cheaper and faster as compared to other seismic methods like MASW. To estimate the thickness of the soil column above bedrock, seismic data were collected in active and passive mode.

The HVSr analysis of ambient noise from passive records provided different typologies of HVSr peaks which enabled us to infer the presence of subsurface heterogeneities. The central part of the valley has clear peaks indicating sharp contrast between the soft alluvium and hard substratum, whereas multiple peaks were mainly observed from northern and southern fringes of the basin and along the fault zones, reflecting lithological complexities underneath. The multiplicity of HVSr peaks is inferred to be related

with the presence of more levels of impedance contrast and implies a greater damage potential because different frequency peaks at the same site may cause amplifications at multiple frequencies during strong motion excitation. The same phenomenon has also been observed in the Kathmandu Valley by Paudyal et al. (2012). Broad peaks were observed from the sites with sloping interface between different strata (SESAME 2004). Most of the sites in the Kangra Valley are mainly characterized by the presence of fan sediments (boulder, cobbles and sand with clay as matrix material) underlain by Upper Siwalik Boulder Conglomerates or Middle and Lower Siwalik Sandstone or Dharamsala Group (sandstone, mudstone and claystone). Hence, the material composition of the overburden material is almost the same except the variation in their compaction, because most of the alluvial material is a product of weathering from the same rock. Thus, at places where the underneath bedrock and the overlying material have similar composition, the HVSr curve is found to present low spectral ratios and flat HVSr curve, reflecting very poor contrast (Tun et al. 2016; Mahajan and Kumar 2018).

Since, the HVSr analysis only provides the fundamental frequency of each site, a multichannel simulation with one receiver (MSOR) was performed in active mode at some of the sites where the HVSr data were obtained. The active mode allowed us to penetrate up to bedrock with joint-fit-inversion modelling of HVSr and dispersion curve. These multiple simulations along a linear profile allowed to drive a 1-D shear velocity profile to understand the thickness of the soil column above bedrock, which was validated from the MASW results obtained by Mahajan and Kumar (2018). This modelling not only provides 1-D shear wave velocity profile but also provides depth with respect to the main impedance contrast to deduce new empirical relationship from non-linear regression analysis.

Since, the Kangra Valley is highly rugged and it is often impossible to deploy linear profiles using MSOR technique

or any other seismic reflection method, because most of the sites are inaccessible, ambient noise measurements were used to determine overburden characteristics from the fundamental frequency of each site. To determine the thickness of the surface layer at such sites, the new empirical relationship derived from experimental data by taking input from joint-fit-inversion modelling, i.e. $H(\text{MSOR}) = 183.13f_0^{-1.542}$ (Eq. 7) between frequency and thickness derived from MSOR data, were utilized to derive sediment thickness from 200 sites. This relationship can also be used for estimating the thickness of sediment above bedrock where only resonance frequency is available. Thus, the present study will be very useful in conducting site characterization studies in other parts of the frontal Himalayan region and areas with young sedimentary basin.

Acknowledgements The authors are thankful to Central University of Himachal Pradesh (CUHP) for providing basic logistic. The financial grant provided by the Ministry of Earth Sciences, Govt. of India, under the project no. MoES/P.O.(Seismo)/1(206)/2013 is thankfully acknowledged. The authors also acknowledge the feedback and constructive input from two anonymous reviewers.

References

- Al Yuncha Z, Luzon F (2000) On the horizontal-to-vertical spectral ratio in sedimentary basins. *Bull Seism Soc Am* 90(4):1101–1106
- Ambraseys NN, Douglas J (2004) Magnitude calibration of north Indian earthquakes. *Geophys J Int* 159(1):165–206. <https://doi.org/10.1111/j.1365-246X.2004.02323.x>
- Bindi D, Parolai S, Spallarossa D, Cattaneo M (2000) Site effects by H/V ratio: comparison of two different procedures. *J Earthq Eng* 4(1):97–113. <https://doi.org/10.1080/13632460009350364>
- Birgoren G, Ozel O, Siyahi B (2009) Bedrock depth mapping of the Coast South of Istanbul: comparison of analytical and experimental analyses. *Turkish J Earth Sci* 18:315–329. <https://doi.org/10.3906/yer-0712-3>
- BIS (2002) IS:1893–2002: criteria for earthquake resistant design of structure. Bureau of Indian Standards, New Delhi
- Bonnefoy-Claudet S, Cotton F, Bard PY (2006) The nature of noise wavefield and its applications for site effects studies. A literature review. *Earth Sci Rev* 79:205–227. <https://doi.org/10.1016/j.earscirev.2006.07.004>
- Castellaro S (2016) The complementarity of H/V and dispersion curves. *Geophysics* 81(6):323–338. <https://doi.org/10.1190/GEO2015-0399.1>
- Castellaro S, Mulargia F (2009) V_{S30} estimates using constrained H/V measurements. *Bull Seismol Soc Am* 99:761–773. <https://doi.org/10.1785/0120080179>
- Chan CH, Wang Y, Almeida R, Yadav RBS (2017) Enhanced stress and changes to regional seismicity due to the 2015 Mw 7.8 Gorkha, Nepal, earthquake on the neighbouring segments of the main Himalayan thrust. *J Asian Earth Sci* 133(1):46–55. <https://doi.org/10.1016/j.jseaes.2016.03.004>
- Dey S, Thiede RC, Schildgen TF, Wittmann H, Bookhagen B, Scherler D, Strecker MR (2016) Holocene internal shortening within the northwest Sub-Himalaya: out-of-sequence faulting of the Jwalamukhi thrust, India. *Tectonics* 35:2677–2697. <https://doi.org/10.1002/2015TC004002>
- Fah D, Kind F, Giardini D (2001) A theoretical investigation of average H/V ratios. *Geophys J Int* 145(2):535–549. <https://doi.org/10.1046/j.0956-540x.2001.01406.x>
- Gabas A, Macau A, Benjumea B, Bellmunt F, Figueras S, Vila M (2014) Combination of geophysical methods to support urban geological mapping. *Surv Geophys* 35:983–1002. <https://doi.org/10.1007/s10712-013-9248-9>
- Gautam D (2017) Unearthed lessons of 25 April 2015 Gorkha earthquake (Mw 7.8): geotechnical earthquake engineering perspectives. *Geomat Nat Haz Risk* 8(2):1358–1382. <https://doi.org/10.1080/19475705.2017.1337653>
- Gupta RK, Agrawal M, Pal SK, Kumar R, Srivastava S (2019) Site characterization through combined analysis of seismic and electrical resistivity data at a site of Dhanbad, Jharkhand. *India Environ Earth Sci* 78:226. <https://doi.org/10.1007/s12665-019-8231-2>
- Harutoonian P, Leo CJ, Tokeshi K, Doanh T, Castellaro S, Zou JJ, Liyanapathirana DS, Wong H (2013) Investigation of dynamically compacted ground by HVSR-based approach. *Soil Dyn Earthq Eng* 46:20–29. <https://doi.org/10.1016/j.soildyn.2012.12.004>
- Ibs-von Seht MIV, Wohlenberg J (1999) Microtremor measurements used to map thickness of soft sediments. *Bull Seismol Soc Am* 89(1):250–259
- Jayangondaperumal R, Kumahara Y, Thakur VC et al (2017) Great earthquake surface ruptures along backthrust of the Janauri anticline, NW Himalaya. *J Asian Earth Sci* 133:89–101. <https://doi.org/10.1016/j.jseaes.2016.05.006>
- Kanai K (1961) An empirical formula for the spectrum of strong earthquake motions. *Bull Earthq Res Inst Univ Tokyo* 39:85–95
- Kanai K, Tanaka T (1961) On microtremors. *VIII Bull Earthq Res Inst* 39:97–114
- Konno K, Ohmachi T (1998) Ground-motion characteristics estimated from spectral ratio between horizontal and vertical components of microtremor. *Bull Seism Soc Am* 88(1):228–241
- Kramer SL (1996) *Geotechnical Earthquake Engineering*, 1st edn. Prentice Hall, Upper Saddle River, p 653
- Lin S, Ashlock JC (2016) Surface-wave testing of soil sites using multichannel simulation with one-receiver. *Soil Dyn Earthq Eng* 87:82–92. <https://doi.org/10.1016/j.soildyn.2016.04.013>
- Lunedei E, Malischewsky P (2014) A review and some new issues on the theory of the H/V technique for ambient vibrations. *Geotech Geol Earthq Eng* 34:371–394. <https://doi.org/10.1007/978-3-319-07118-3>
- Mahajan AK (2009) NEHRP soil classification and estimation of 1-D site effect of Dehradun fan deposits using shear wave velocity. *Eng Geol* 104:232–240. <https://doi.org/10.1016/j.enggeo.2008.10.013>
- Mahajan AK, Kumar S (1994) Linear features registered on the Landsat imagery in the Dharamsala-Palampur area NW Himalaya, vis-à-vis seismic status of the area. *Geophysika* II:15–25
- Mahajan AK, Kumar P (2018) Site characterisation in Kangra Valley (NW Himalaya, India) by inversion of H/V spectral ratio from ambient noise measurements and its validation by multi-channel analysis of surface waves technique. *Near Surf Geophys* 16(3):314–327. <https://doi.org/10.3997/1873-0604.2018008>
- Mahajan AK, Kumar N, Arora BR (2006) Quick isoseismal map of 8th October, 2005 Kashmir earthquake. *Curr Sci* 91(3):356–361
- Mahajan AK, Thakur VC, Sharma ML, Chauhan M (2010) Probabilistic seismic hazard map of NW Himalaya and its adjoining area, India. *Nat Hazards* 53:443–457. <https://doi.org/10.1007/s11069-009-9439-3>
- Middlemiss CS (1910) The Kangra earthquake of 4th April, 1905. *Mem Geol Surv India* 38:1–409
- Mucciarelli M, Gallipoli MR (2001) A critical review of 10 years of microtremor HVSR technique. *Boll Geofis Teor Appl* 42(3–4):255–266

- Nakamura Y (1989) A method for dynamic characteristics estimation of subsurface using microtremor on the ground surface. *Q Rep Railw Tech Res Inst* 30(1):25–33
- Nakamura Y (2000) Clear identification of fundamental idea of Nakamura's technique and its application. In: *Proceedings of the 12th world conference on earthquake engineering*, Auckland, New Zealand, pp 8
- Nogoshi M, Igarashi T (1971) On the amplitude characteristics of microtremor (part 2). *J Seismol Soc Japan* 24:26–40
- Ori GG, Friend PF (1984) Sedimentary basins formed and carried piggyback on active thrust sheets. *Geol* 12:475–478. [https://doi.org/10.1130/0091-7613\(1984\)12%3c475:SBFACP%3e2.0.CO;2](https://doi.org/10.1130/0091-7613(1984)12%3c475:SBFACP%3e2.0.CO;2)
- Ozalaybey S, Zor E, Ergintav S, Tapırdamaz MC (2011) Investigation of 3-D basin structures in the İzmit Bay area (Turkey) by single-station microtremor and gravimetric methods. *Geophys J Int* 186:883–894. <https://doi.org/10.1111/j.1365-246X.2011.05085.x>
- Park CB, Miller RD, Xia J (1999) Multichannel analysis of surface waves. *Geophysics* 64(3):800–808
- Peralai S, Bormann P, Milkereit C (2002) New relationships between vs, thickness of sediments, and resonance frequency calculated by the H/V ratio of seismic noise for the cologne area (Germany). *Bull Seismol Soc Am* 92(6):2521–2527
- Paudyal YR, Yatabe R, Bhandary NP, Dahal RK (2012) A study of local amplification effect of soil layers on ground motion in the Kathmandu Valley using microtremor analysis. *Earthq Eng Eng Vib* 11(2):257–268. <https://doi.org/10.1007/s11803-012-0115-3>
- Paudyal YR, Yatabe R, Bhandary NP, Dahal RK (2013) Basement topography of the Kathmandu Basin using microtremor observation. *J Asian Earth Sci* 62:627–637. <https://doi.org/10.1016/j.jseae.2012.11.011>
- Rezaei S, Choobbasti AJ (2017) Application of the microtremor measurements to a site effect study. *Earthq Sci* 30(3):157–164. <https://doi.org/10.1007/s11589-017-0187-2>
- Rezaei S, Choobbasti AJ, Kutanaei SS (2013) Site effect assessment using microtremor measurement, equivalent linear method, and artificial neural network (case study: Babol, Iran). *Arab J Geosci* 8(3):1453–1466. <https://doi.org/10.1007/s12517-013-1201-1>
- Rix GJ, Leipski EA (1991) Accuracy and resolution of surface wave inversion. In: Bhatia SK, Blaney GW (eds) *Recent advances in instrumentation, data acquisition and testing in soil dynamics*. American Society of Civil Engineers, Reston, pp 17–32
- Roser J, Gosar A (2010) Determination of V_{s30} for seismic ground classification in the Ljubljana area, Slovenia. *Acta Geotech Slov* 7:61–76
- Ryden N, Park CB, Ulriksen P, Miller RD (2004) Multimodal approach to seismic pavement testing. *J Geotech Geoenviron Eng* 130:636–645. [https://doi.org/10.1061/\(ASCE\)1090-0241\(2004\)130:6\(636\)](https://doi.org/10.1061/(ASCE)1090-0241(2004)130:6(636))
- Sah MP, Srivastava RAK (1992) Morphology and facies of the alluvial-fan sedimentation in the Kangra Valley. *Himachal Himalaya Sediment Geol* 76(1–2):23–42
- SESAME (2004) Guidelines for the implementation of the H/V spectral ratio technique on ambient vibrations, Rapport final
- Tarabusi G, Caputo R (2016) The use of HVSr measurements for investigating buried tectonic structures: the Mirandola anticline, Northern Italy, as a case study. *Int J Earth Sci* 106:341–353. <https://doi.org/10.1007/s00531-016-1322-3>
- Te CC, Chang SC, Wen KL (2017) Stochastic ground motion simulation of the 2016 Meinong, Taiwan earthquake. *Earth Planets Sp* 69:62. <https://doi.org/10.1186/s40623-017-0645-z>
- Thakur VC, Joshi M, Sahoo D, Suresh N, Jayangondapermal R, Singh A (2014) Partitioning of convergence in Northwest sub-Himalaya: estimation of late Quaternary uplift and convergence rates across the Kangra reentrant, North India. *Int J Earth Sci* 103:1037–1056. <https://doi.org/10.1007/s00531-014-1016-7>
- Tokeshi K, Harutoonian P, Leo CJ, Liyanapathirana S (2013) Use of surface waves for geotechnical engineering applications in Western Sydney. *Adv Geosci* 35:37–44. <https://doi.org/10.5194/adgeo-35-37-2013>
- Tun M, Pekkan E, Ozel O, Guney Y (2016) An investigation into the bedrock depth in the Eskisehir Quaternary Basin (Turkey) using the microtremor method. *Geophys J Int* 207(1):589–607. <https://doi.org/10.1093/gji/ggw294>

Publisher's Note Springer Nature remains neutral with regard to jurisdictional claims in published maps and institutional affiliations.